LBL-36369
UC-414

Lawrence Berkeley Laboratory

UNIVERSITY OF CALIFORNIA

Accelerator & Fusion Research Division

Presented at the Sixth Workshop on Advanced Accelerator Concepts, Lake Geneva, WI, June 12–18, 1994, and to be published in the Proceedings

Femtosecond X-ray Generation through 90° Thomson Scattering: Status of the LBL Experiment

W. Leemans, R. Schoenlein, A. Chin, E. Glover, M. Conde, S. Chattopadhyay, K.-J. Kim, and C.V. Shank

November 1994

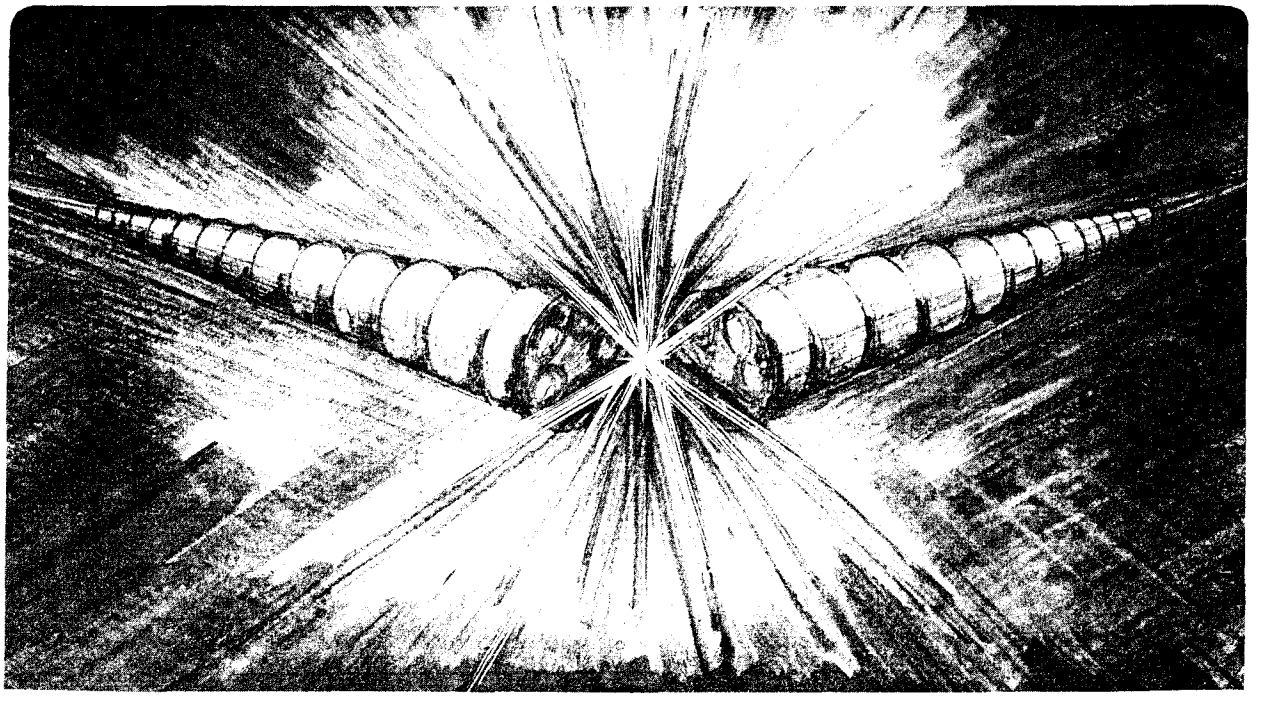

LOAN COPY
Circulates
for 4 weeks
Bldg. 50 Library.
Copy 2
LBL-36369

Prepared for the U.S. Department of Energy under Contract Number DE-AC03-76SF00098

LBL-36369
CBP Note-107

Femtosecond X-ray Generation through 90° Thomson Scattering: Status of the LBL Experiment*

W. Leemans, R. Schoenlein, A.Chin, E. Glover, M. Conde,
S. Chattopadhyay, K.-J. Kim, and C.V. Shank

Lawrence Berkeley Laboratory
University of California
Berkeley, CA 94720

* This work was supported by the Director, Office of Energy Research, Office of High Energy and Nuclear Physics, High Energy Physics Division, of the U.S. Department of Energy under Contract No. DE-AC03-76SF00098.

Femtosecond X-ray Generation through 90° Thomson Scattering: Status of the LBL Experiment*

W. Leemans, R. Schoenlein, A. Chin, E. Glover, M. Conde,
S. Chattopadhyay, K.- J. Kim, and C. V. Shank
Lawrence Berkeley Laboratory
1 Cyclotron Road, Berkeley, CA 94720 USA

Abstract: Scattering of femtosecond laser pulses off a low energy relativistic electron beam at 90° offers the possibility to generate ultrashort X-ray pulses. Experiments are under preparation in the Beam Test Facility of the Center for Beam Physics at LBL to demonstrate the generation and detection of such pulses. The experiments involve a relativistic electron beam (tunable from 25 - 50 MeV) with a bunch length of 10 ps containing 1 -2 nC, and an ultra short pulse (50 - 200 fs), high peak power (> 2 TW) 0.8 μm Ti:Al_2O_3 laser system. The electron beam, focused down to about a 50 μm waist size intersects the focused laser beam at 90°. The laser field acts as an electromagnetic undulator with strength K (quiver velocity of an electron normalized to the speed of light) for the relativistic electron beam, generating radiation up-shifted by $2\gamma^2/(1+K^2/2)$ and a pulse length given by the overlapped interaction length in time of the laser beam and the electron beam. Here γ is the usual Lorentz factor. Wavelength tuning will be accomplished in the experiment by generating wiggler strengths on the order of one as well as by electron beam energy tuning. For a 50 MeV electron beam and a laser beam focused to an intensity on the order of 10^{16} W/cm^2, we expect 10^5 photons at 0.4 Å (10% bandwidth) in a cone angle of 6 mrad in a 170 fs pulse.

INTRODUCTION

A scientific frontier of great importance to studies of all ultrafast phenomena and of immediate relevance to basic and industrial applications in surface, material, chemical and biological sciences, is the generation and use of femtosecond X-ray pulses. Such a source will allow direct measurements of the structure of materials on a time scale comparable to a vibrational period, i.e. time resolve atomic motion. This will provide valuable information about the properties of novel materials as well as important chemical and biological reactions occurring on ultrafast time scales.

Our goal is to develop and test a technically feasible concept and the associated technology for the production of ultrashort X-ray pulses with a

* This work was supported by the Director, Office of Energy Research, Office of High Energy and Nuclear Physics, High Energy Physics Division, of the U.S. Department of Energy under Contract No. DE-AC03-76SF00098.

performance reach to the regime of 1 Å, 30 fs and 10^{12} photons/s, which we believe will have wide-scale scientific and industrial utility. The proposed approach consists of generating femtosecond X-ray pulses via right angle Thomson scattering [1] a near-infrared, terawatt femtosecond laser against a moderate energy (25 - 50 MeV) tightly focused electron beam [2], [3].

The interaction of laser beams and relativistic electron beams has also gained great importance for high energy physics : γ - γ colliders will rely on high power lasers scattering off relativistic electron beams; laser based diagnostics have been proposed and developed [2] to determine the transverse and longitudinal properties of electron beams at the final focus in high energy colliders.

Laser Undulators

Using a laser beam as an electromagnetic undulator has been proposed in the early 60s by Milburn and Arutyunian and V.A. Tumanian [5]. Subsequently experiments on synchrotrons [6], linacs [7] and storage rings [8] were reported. In those original experiments the photon flux was typically extremely low. The availability of chirped pulse amplification (CPA) [9] based compact terawatt lasers renewed the interest in the use of lasers as undulators and spawned lots of theoretical work on laser undulator based light sources (backscatter geometry) and non-linear Thomson scattering [10]. In the backscattering geometry the pulse length is determined by the longer of the laser or electron pulse (typically the latter). Femtosecond long X-ray pulses can be generated by using femtosecond optical laser pulses and colliding them with a relativistic electron beam at 90°[1]. In this geometry the X-ray pulse length is determined by the longer of the laser pulse and the transit time of the laser beam across the electron beam waist. The details of this X-ray source will be discussed below.

Laser Pumped and Synchrotron X-ray Sources

X-ray sources based on the interaction of terawatt laser pulse with solids have recently demonstrated high efficiency in the sub-keV region [11]. However, the efficiency rapidly decreases for higher energy X-ray radiation and plasma dynamics may prevent femtosecond pulse lengths. Harmonic generation in gases [12] has been shown to produce highly directional and coherent light with duration on the order of the incident pulse. The shortest wavelength generated to date is however is on the order of 50 Å with efficiencies on the order of 10^{-11}. Third generation light sources such as the Advanced Light Source (ALS) [13] at Lawrence Berkeley Laboratory and the Advanced Photon Source (APS) [14] at Argonne National Laboratory generate high brightness, high peak and average power, tunable X-ray radiation but pulse lengths are typically 30 - 40 ps.

ORTHOGONAL THOMSON SCATTERING

A first estimate of the laser and electron beam requirements can be made using a simple Thomson scattering model:

$$\frac{X-rays}{pulse} = \frac{incident\ photons}{pulse\ cm^2}\sigma_T n_e \frac{\sigma_L}{\sigma_e} \tag{1}$$

where σ_T is the Thomson cross-section, n_e the number of electrons per bunch, σ_L and σ_e the duration of the laser pulse and electron bunch respectively. For typical electron beam parameters (1 nC/bunch, bunch length σ_e about 10 ps) and laser beam parameters (pulse length σ_L of 150 fs, 150 mJ/pulse) and matching the transverse electron beam size (i.e. transit time) to the laser pulse length we estimate to produce 10^5 X-rays per pulse. The generic set-up is shown in Fig. 1.

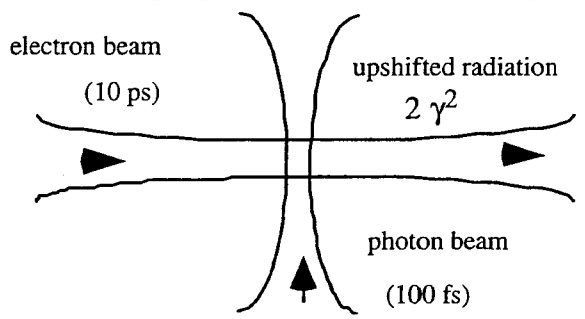

FIGURE 1. Generic lay-out of the 90 X-ray generation experiment. The laser beam is up-shifted by $2\gamma^2$ and propagates in the direction of the electron beam.

We next determine the relevant properties of the scattered radiation such as the expected wavelength shift, number of photons per pulse, pulse duration, and the spectral width.

The frequency of the up-shifted radiation can easily be calculated from energy and momentum conservation:

$$\omega_r = \frac{\gamma_{eff}\omega_o}{\gamma_{eff}(1-\beta\cos\theta) + \frac{\hbar\omega_o}{mc^2}(1-\sin\theta)} \tag{2}$$

and

$$\gamma_{eff} = \frac{\gamma}{\sqrt{1 + K^2/2}} \tag{3}$$

Here β and γ are the normalized velocity and Lorentz factor, θ the angle of observation, ω_0 the incident laser frequency, c the speed of light, m the electron rest mass. The undulator strength K is given by

$$K = \frac{25.6}{c[cm/s]}\sqrt{I[W/cm^2]}\lambda[\mu m] \tag{4}$$

where I is the incident laser intensity and λ the wavelength. In our experiment the Compton shift can be neglected and θ is small so that Eqn. (2) reduces to

$$\omega_r \cong \frac{2\gamma^2\omega_o}{1 + K^2/2 + \gamma^2\theta^2} \tag{5}$$

The number of photons per pulse, taking into account the proper Gaussian temporal and spatial profiles of both the electron and laser beam can be found from [1]:

$$\Delta n = \pi\alpha K^2 N_{eff} n_e \frac{\Delta\lambda}{\lambda} \frac{\sigma_w\sqrt{\sigma_w^2 + \sigma_L^2}}{\sqrt{(\sigma_x^2 + \sigma_w^2)(\sigma_z^2 + \sigma_x^2 + \sigma_w^2 + \sigma_L^2)}} \tag{6}$$

Here N_{eff} is the effective number of undulator periods with which the electron beam interacts:

$$N_{eff} = \frac{2\sqrt{\pi}}{\lambda_L} \frac{\sigma_w\sigma_L}{\sqrt{\sigma_w^2 + \sigma_L^2}} \tag{7}$$

The X-ray pulse duration is then given by (for $\sigma_Z >> \sigma_X$)

$$\tau_X = \frac{\sqrt{\sigma_x^2 + \sigma_w^2 + \sigma_L^2}}{\sqrt{1 + \frac{(\sigma_x^2 + \sigma_w^2 + \sigma_L^2)}{\sigma_z^2}}} \tag{8}$$

with σ_X, σ_Z the transverse and longitudinal electron beam sizes and σ_W, σ_L the laser transverse and longitudinal laser beam sizes (in microns). Further simplification of Eqn.(6) leads to

$$\Delta n = 113\frac{\Delta\lambda}{\lambda} J n_e \frac{\lambda_L}{\sqrt{(\sigma_x^2+\sigma_w^2)(\sigma_z^2+\sigma_x^2+\sigma_w^2+\sigma_L^2)}} \tag{9}$$

where J is the laser energy in Joules. The number of photons per electron within a given bandwidth is therefore independent of γ whereas the energy efficiency increases with γ.

The spectral width within a cone of half angle θ is

$$\frac{\Delta\omega}{\omega} \cong \gamma^2\theta^2 \tag{10}$$

Bandwidth broadening is caused by a variety of mechanisms:
(a) finite interaction length broadening

$$\left.\frac{\Delta\omega}{\omega}\right|_i \cong \frac{1}{N_{eff}} \tag{11}$$

(b) energy spread broadening

$$\left.\frac{\Delta\omega}{\omega}\right|_E \cong 2\frac{\Delta\gamma}{\gamma} \tag{12}$$

(c) finite emittance broadening

$$\left.\frac{\Delta\omega}{\omega}\right|_\varepsilon \cong \gamma^2\theta^2 = \frac{\varepsilon_n^2}{\sigma_x^2} \tag{13}$$

and
(d) laser bandwidth broadening

$$\left.\frac{\Delta\omega}{\omega}\right|_{\sigma_L} \cong \frac{\Delta\omega_o}{\omega_o} = \frac{4\ln 2\lambda_L}{2\pi\sigma_L} \tag{14}$$

Here ε_n is the normalized emittance. The total broadening is then given by

$$\left.\frac{\Delta\omega}{\omega}\right|_T = \sqrt{\left(\left.\frac{\Delta\omega}{\omega}\right|_i\right)^2 + \left(\left.\frac{\Delta\omega}{\omega}\right|_E\right)^2 + \left(\left.\frac{\Delta\omega}{\omega}\right|_\varepsilon\right)^2 + \left(\left.\frac{\Delta\omega}{\omega}\right|_{\sigma_L}\right)^2} \tag{15}$$

EXPERIMENT

The current experiment at LBL involves the use of a 50 MeV electron beam and a terawatt Ti:Al_2O_3 laser system in the Beam Test Facility (BTF) [2], [3]. We next give a brief description of the BTF and the laser system. The lay-out of the BTF-line is shown in Fig. 2

The Beam Test Facility.

The BTF, operated under the auspices of the Center for Beam Physics at Lawrence Berkeley Laboratory in support of its experimental R&D program, is located inside the ALS complex. The ALS has a 50 MeV linac, a booster ring which increases the electron energy to 1.5 GeV and a storage ring which typically needs refilling every 6 - 8 hours. The ALS linac parameters are given in Table 1.

TABLE 1. ALS linac parameters.

Maximum energy	50 MeV
Charge	1-2 nC/bunch
Bunch length (σ_z)	10-15 ps
Emittance rms. (unnorm)	0.35 mm-mrad
number of bunches/macropulse @ 125 MHz	1 - 10 (max. 100)
Macropulse repetition rate	1 - 10 Hz

In between refills the 50 MeV electron beam can be transported into the BTF. A variety of experiments are planned involving the interaction of such a relativistic electron beam with plasmas (plasma focusing, advanced accelerator concepts), laser beams (generation of femtosecond X-ray pulses) and electromagnetic cavities (Crab cavities etc.....). The beam line is designed using the measured emittance and Twiss parameters of the ALS linac. It can accommodate the different requirements imposed by the various experiments on the electron beam properties (charge, energy, pulse length) and on the handling of the beam before and after the interaction points.

The electron beam is transported to the interaction point using two achromatic bending sections (BX through B2 and B3 through B4) and is focused using Q7 (a 6.25 cm diameter quadrupole triplet) and Q8 (a 15 cm diameter quadrupole triplet) inside a vacuum chamber where the interaction with the laser beam takes

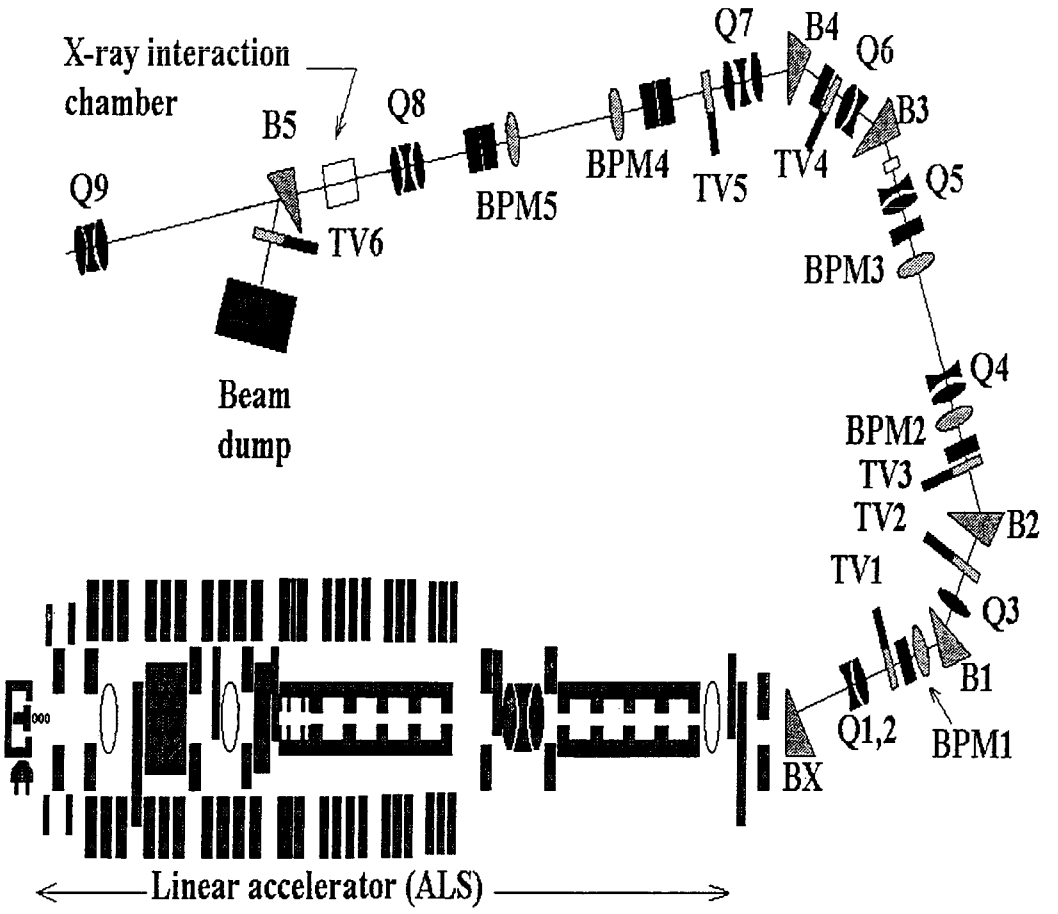

FIGURE 2. Lay-out of the BTF-line. The bending magnets are labeled B1 through B5 and the quadrupole magnets are labeled Q1 through Q9. The location of beam position monitors and fluorescent screens are denoted by BPM1 through 5 and TV1 through 6 respectively. Optical Transition Radiation diagnostic systems are currently installed between Q5 and B3 and between Q8 and B5.

place. The beam is then deflected inside a shielded beam dump using the B5 magnet.

A wide range of diagnostics have been built and implemented to allow full characterization of the electron beam. These include integrating current transformers for charge measurement, high bandwidth beam position monitors, fluorescent screens for transverse beam analysis and an optical transition radiation (OTR) diagnostic system [15]. Typical electron beam spots along the BTF-line as monitored by fluorescent screens are shown in Fig. 3.

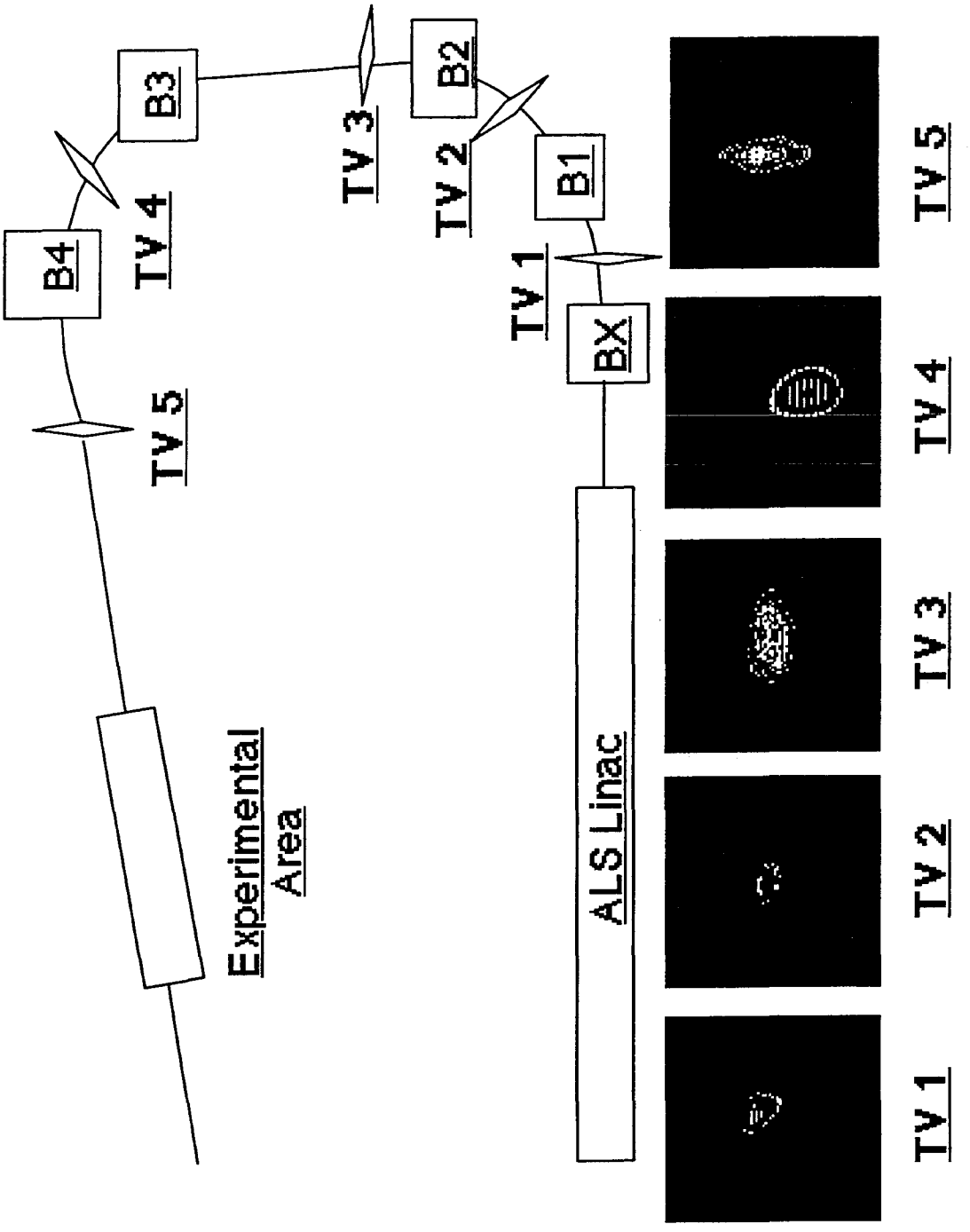

FIGURE 3. Electron beam spots along the BTF-line as monitored by fluorescent screens.

The OTR system allows single bunch measurement of beam emittance, energy, charge and bunch length [15]. The radiator is made of a 2 μm thick nitrocellulose foil coated with 350 nm thick aluminum. Using a small f-number optical telescope system, the radiation is transported out of the shielded vault onto a cooled slow scan 16 bit CCD camera. A typical electron beam spot (proximity focus) with horizontal and vertical line-out and radiation cone (infinity focus) with horizontal line-out are shown in Figs. 4 (a,b,c) and 5(a,b) respectively. The horizontal (vertical) electron beam size is obtained by fitting a Gaussian function through a horizontal (vertical) line-out through the center of the spot. The horizontal (vertical) beam divergence is obtained as follows. The shape of the radiation cone is determined by a convolution of a single electron radiation profile and a Gaussian distribution for the angles of incidence of the electrons on the foil.

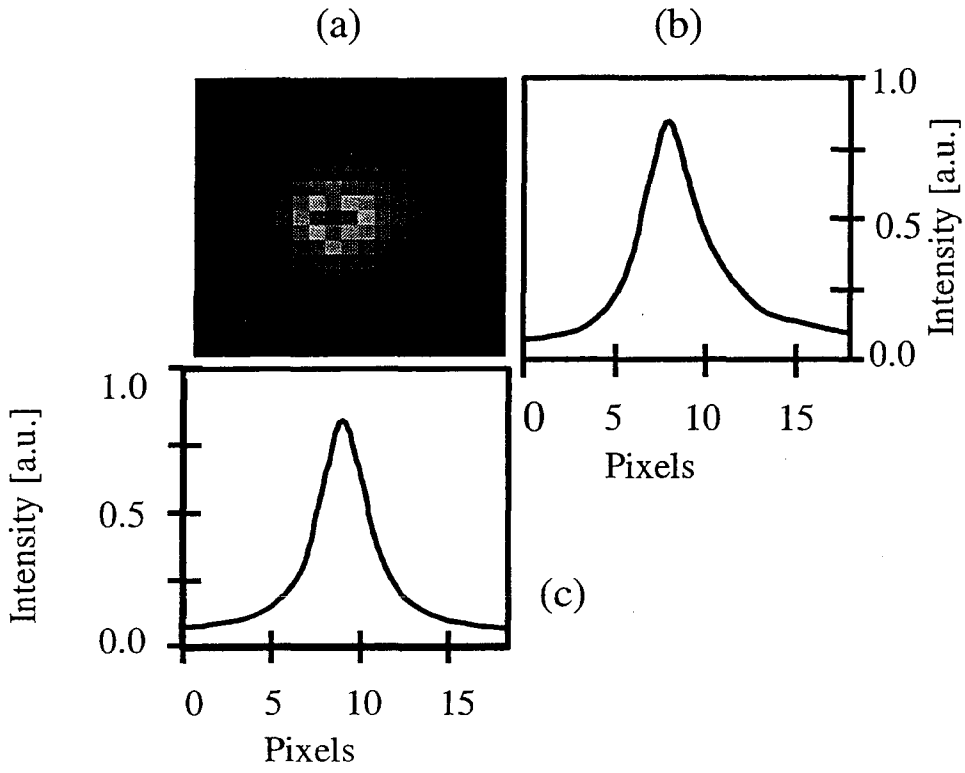

FIGURE 4. (a) OTR image of the electron beam spot inside the X-ray interaction chamber with vertical (b) and horizontal (c) line-out. The actual spot size is probably less than the measured spot size σ_x = 115 as the present optical lens system is resolution limited to about 100 μm.

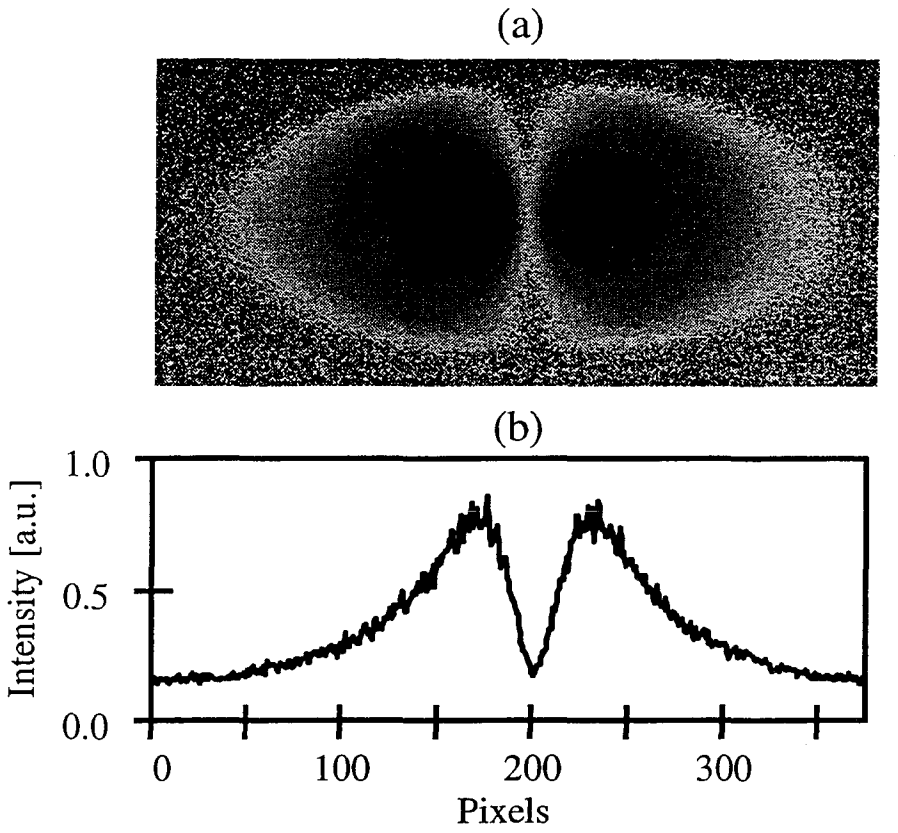

FIGURE 5. A typical OTR image of the radiation cone (a) and a horizontal line-out (b). A polarizer was used to minimize the contribution of the vertical electron beam divergence.

To achieve the required X-ray pulse duration, the electron beam will be focused down to a spot size of 35 μm using a telescope consisting of two quadrupole triplets. The large bore (6") of the final magnet allows for small f-number focusing and minimizes Bremsstrahlung production by beam halo scraping against the beam pipe. A 60° H-magnet separates the particle and photon beams after the interaction point.

The OTR image shown in Fig. 4 is an image of the electron beam spot inside the X-ray interaction chamber. At present a spot size less than 100 μm has been measured.

Laser System

The lay-out of the laser system is shown in Fig. 6 and the main laser system parameters are listed in Table 2. The laser system is located on top of the

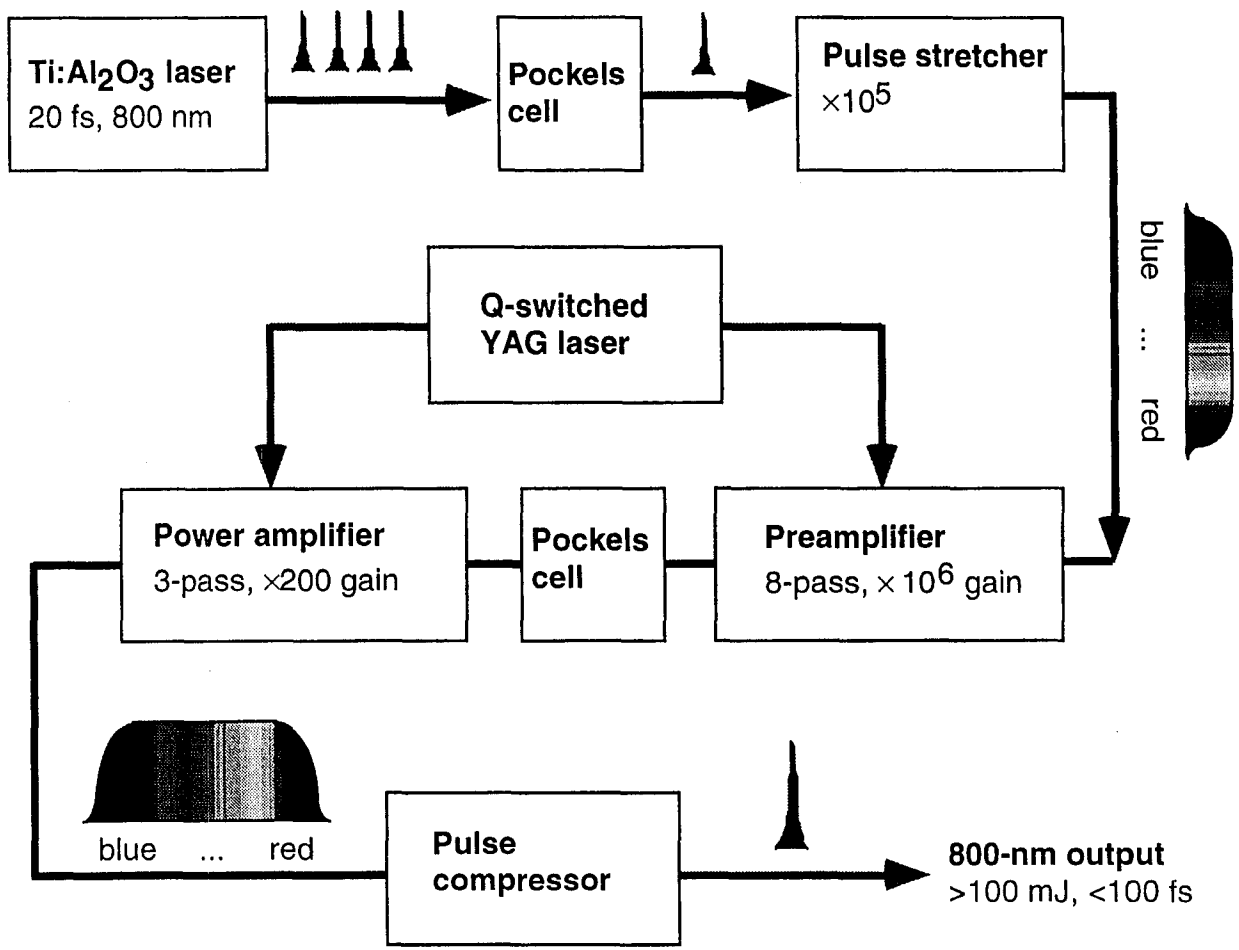

FIGURE 6. Lay-out of the laser system.

electron transport line shielding blocks. The passively Kerr lens modelocked $Ti:Al_2O_3$ laser oscillator operates at 125 MHz (4th subharmonic of the ALS 500 MHz linac masterclock frequency) and generates 20 fs long pulses each containing about 2 nJ. Individual pulses from the oscillator are selected out at a 10 Hz rate using a Pockel cell and stretched a factor $\sim 10^4$ using a grating pair. An 8-pass preamplifier with $\sim 10^6$ gain and a 3 pass main amplifier with ~100 gain amplify the pulse to an energy of >200 mJ. The pulse is then compressed in vacuum using a second grating pair, yielding a final pulse duration of 50 fs with energies in excess of 125 mJ.

TABLE 2. Laser system parameters

Wavelength	0.8 μm
Energy/pulse	125 mJ
Pulse length	50 - 200 fs
Repetition rate	10 Hz
Timing jitter with RF	< 2 ps

An evacuated laser beam delivery system transports the laser beam through a hole in the radiation shielding into the X-ray interaction chamber (horizontal plane). Initial experiments will use a beam focused to a 35 - 50 μm spot, matching the electron beam transverse dimensions. The peak laser intensity is then on the order of 10^{16} W/cm^2. Pre-alignment of the two beams will be done at low power. Two pairs of horizontal and vertical correctors allow for accurate positioning of the electron beam. The laser and e-beam alignment tolerances put tight constraints on the shot-to-shot movement of the beam in the transverse and longitudinal directions. The effect of current ripple in the power supplies of the bend magnets and the quadrupoles on the beam dynamics has been modeled previously [2] and preliminary measurements indicate that pointing accuracy of the electron beam is better than 50 μm.

From Eqn. (5) it can be seen that wavelength tuning can be accomplished by changing the electron beam energy γ, the angle of observation θ or the wiggler strength K. Although the ALS linac can be operated at energies lower than 50 MeV, the most straightforward option by far for wavelength tuning in our experiment is changing the size of the focused laser beam. For $\sigma_x >> \sigma_w, \sigma_L$ Eqn. (9) shows that the number of scattered photons depends only on the laser energy. By focusing the laser beam to a 4 - 5 μm spot size, laser intensities on the order of 4 - 5 x 10^{18} W/cm^2 will be achieved giving a wiggler strength on the order of K = 1.36. The expected X-ray wavelength using the 50 MeV electron beam will then be on the order of 1.1 Å (11 keV). In addition, the large wiggler strength will lead to the generation of harmonics [10].

Since the length of the electron beam bunch σ_z is on the order of 10 - 15 ps, temporal overlap between the two pulses should not pose any great difficulty. In fact, we have achieved RF locking of the laser oscillator to a 500 MHz RF clock with timing jitter performance better than 2 ps.

X-ray Source Parameters and Diagnostics

The X-ray source parameters are given in Table 3. The parameters have been calculated using Eqns. (5) and (7) through (11) with electron and laser beam parameters from Tables 1 and 2.

TABLE 3. X-ray source parameters. The wavelength and cone angle values are calculated for a 50 MeV electron beam energy and a laser intensity of 10^{16}W/cm^2. The large value for the source brightness is due to its very small size.

Wavelength (Å)	0.4
Pulse length (fs)	200
number of photons (10 % bandwidth)	1.3×10^5
Full angle cone (mrad)	6
Bandwidth (%)	80 %
Repetition rate	1 Hz
Peak power	3 kW
Average power	0.6 nW
Brightness photons/(s mm^2 mrad^2 0.1% bandwidth)	1.7×10^{19}

A variety of X-ray diagnostics will be implemented to measure wavelength, beam size and divergence, pulse length and polarization.

A 75 μm Be-foil isolates the beam line high vacuum from the X-ray diagnostic systems. Detailed calculations have been performed to estimate the required amount of shielding to reduce the background X-ray level, caused by the close proximity of the beam dump to the X-ray diagnostic, below 10 photons/cm^2 (total spectrum). Spatial filtering with a tapered lead cone pointing at the laser electron beam interaction volume will reduce the number of Bremsstrahlung X-rays co-propagating with the beam.

Spatial properties of the X-ray beam (spot size and divergence) will be measured using a slow scan CCD camera looking at a phosphor screen. The photon energy will be determined by using Si(Li) detectors and operating an X-ray CCD camera in a single photon regime. For initial pulse length measurements the transit time will be lengthened by changing the horizontal focusing strength of the quadrupoles, allowing the use of a diamond photodiode as well as an X-ray streak camera. A cross-correlation technique [16] between the X-ray pulse and an optical pulse in a gas jet will be used to measure shorter pulse durations. In the absence of the laser, photo electrons will be produced in a

Kr gas jet by X-rays with energy about 500 eV higher than the K-shell energy of Kr-gas (14.3 keV). In the presence of a high-intensity laser pulse, the X-ray photo electrons will acquire an additional drift velocity component, whose magnitude and direction depends on the phase and amplitude of the laser field at which the photo electron is born and the relative polarization of the laser with respect to the X-rays. The continuum states are effectively AC Stark shifted by an amount corresponding to the ponderomotive energy of the laser. The shift in the photo-electron spectrum as a function of the relative delay between the X-ray pulse and the 0.8 μm laser pulse will provide a cross-correlation measurement from which the X-ray pulse duration can be determined.

SUMMARY

A status report has been given of the planned orthogonal Thomson scattering experiment at the BTF. Based on simple scaling laws we have calculated that about 10^5 X-ray photons will be produced in a 150 - 200 fs long pulse. Both the electron beam line and the laser system have been completed and integration of these systems is well underway. Initial experiments will concentrate on full characterization of the X-ray source parameters. Planned experiments with the X-ray source include a time-resolved X-ray diffraction study of melting in silicon on femto-second time scales and time resolved EXAFS [17].

ACKNOWLEDGMENTS

The authors wish to thank the ALS personnel for their outstanding efforts in the construction of the Beam Test Facility. In particular we would like to acknowledge J. Krupnick, D. Calais and C. Matuk. We also thank R. Govil, M. de Loos, B. vander Geer, Terry Byrne, Glen Ackerman and Ken Luchini for their help during BTF commissioning. One of the authors (W.L.) would also like to thank Dr. E. Esarey for useful discussions.

REFERENCES

[1] K.- J. Kim et al., NIMA 341, 351 (1994).
[2] W. P. Leemans et al., Proc. 1993 Part. Accel Conf, 83 (1993).
[3] W. P. Leemans et al., Proc. 1994 European Part. Accel. Conf, June 1994, London, U.K.
[4] T. Shintake, NIMA 453 (1992).
[5]R. H. Milburn, Phys. Rev. Lett. **10**, 75 (1963); F. R. Arutyunian and V.A. Tumanian, Phys. Lett. **4**, 176 (1963).
[6] O. F. Kulikov et al., Phys. Lett. **13**, 344 (1964); C. Bemporad et al., Phys. Rev. **138**, B1546 (1965).
[7] C. K. Sinclair et al., IEEE Trans. Nucl. Sci. **NS-16**, 1065 (1969)
[8] L. Federici et al., Nuovo Cim. **B59**, 247 (1980); Yamazaki et al., IEEE Trans. Nucl. Sci. **NS-32**, 3406 (1985).

[9] G. Mourou and D. Umstadter, Phys. Fluids **B4**, 2315 (1994) and many references therein.
[10] E. Esarey et al., Phys. Rev E **48**, 3003 (1993) and many references therein.
[11] M. M. Murnane et al., Science **251**, 531 (1991).
[12] A. 'lHuillier and P. Balcou, Phys. Rev. Lett. **70**, 774 (1993).
[13] "1-2 GeV Synchrotron Radiation Source", Conceptual Design Report, LBL-PUB 5172 Rev., 1986.
[14] "Characteristics of the 7 GeV APS", ANL-88-9, 1988.
[15] M. de Loos et al., Proc. 1994 European Part. Accel. Conf, June 1994, London, U.K.
[16] T. Glover et al., Proc. High Field Interactions and Short Wavelength Generation Conference, Aug. 1994, St. Malo, France.
[17] D.C. Koningsberger and R. Prins, ed. *X-ray absorption: principles, applications, techniques of EXAFS, SEXAFS and XANES.* Chemical analysis, ed. J.D. Winefordner, Vol. 92, 1988, Wiley, New-York.